Available online at www.sciencedirect.com

ScienceDirect

Ceramics International 39 (2013) 9459–9464

CERAMICS INTERNATIONAL

www.elsevier.com/locate/ceramint

Sol–gel functionalization of sodium TiO_2 nanotubes and nanoribbons with aminosilane molecules

Ivan Brnardić[a,*], Miroslav Huskić[b,c], Polona Umek[d,e], Tamara Holjevac Grgurić[a]

[a]Faculty of Metallurgy, University of Zagreb, Aleja narodnih heroja 3, 44103 Sisak, Croatia
[b]Center of Excellence PoliMaT, Tehnološki park 24, 1000 Ljubljana, Slovenia
[c]National Institute of Chemistry Slovenia, Hajdrihova 19, 1000 Ljubljana, Slovenia
[d]Jožef Stefan Institute, Jamova cesta 39, 1000 Ljubljana, Slovenia
[e]Center of Excellence Namaste, Jamova 39, 1000 Ljubljana, Slovenia

Received 4 March 2013; received in revised form 11 April 2013; accepted 2 May 2013
Available online 23 May 2013

Abstract

The functionalization of sodium TiO_2 nanotubes and nanoribbons with 3-(aminopropyl)triethoxysilane (APTES) was performed by a sol–gel process using two different methods, namely with and without prehydrolization of APTES. Nanoparticles were functionalized with different amounts of APTES (30, 60 and 100 wt% per nanoparticles) and under different times of functionalization (2, 4 and 24 h). The nature and binding of the APTES molecules on sodium TiO_2 nanoparticles were determined by simultaneous differential scanning calorimetry-thermogravimetric analysis (DSC-TGA), Fourier transform infrared (FTIR) spectroscopy and scanning electron microscopy (SEM) equipped with electron dispersive X-ray spectrometry (EDS). DSC-TGA results showed that the amount of APTES molecules on nanoparticles increased with higher APTES ratios. The existence and binding of the APTES molecules with nanoparticles was confirmed by FTIR and SEM–EDS.

Keywords: A. Sol–gel processes; B. Surfaces; D. TiO_2; Silicate

1. Introduction

In preparation and production of polymer composites, fillers have played an important role from the very beginning of the polymer era. The impact of filler on the physical, chemical and mechanical properties of the polymer depends on the filler's particle distribution in the polymer matrix, the filler/polymer surface interaction and the filler size. With aim to improve those properties, extensive research has been devoted to the field of functionalization of different filler types such as TiO_2 based nanotubes, TiO_2 and SiO_2 nanoparticles, carbon nanotubes, clay and layered silicates etc. [1–11].

In the last decade, 1D nanostructured titanates have been the subject of extensive research due to their large surface area, semi-conducting and catalytic properties [12–15]. These materials can also play an important role as fillers in composites due to their good mechanical properties [16]. Sodium TiO_2 nanotubes (NaTiNTs) and nanoribbons (NaTiNRs) are typically synthesized under hydrothermal conditions [15,17] in gram quantities with high yields from a TiO_2 precursor in an alkaline medium. Typically, NaTiNTs have diameters around 10 nm while their lengths reach up to 500 nm. In contrast, NaTiNRs appear to be much longer, with their lengths reaching up to several microns. A high width-to-height aspect ratio is also characteristic of NaTiNRs. In cross section they can measure up to 150 nm while in height just 20 to 30 nm. In addition, titanate nanostructures are very appealing as a starting material for preparation of 1D TiO_2 nanostructures. This is achieved by an ion-exchange process in acidic media which first results in protonated titanate. During the heat treatment that follows, protonated titanate transforms into TiO_2.

To the best of our knowledge, only a few articles have been published regarding the functionalization of sodium TiO_2 nanotubes [1–3] and preparation of polymer nanocomposites based on functionalized sodium TiO_2 nanotubes or nanoribbons

*Corresponding author at: Faculty of Metallurgy, University of Zagreb, Aleja narodnih heroja 3, 44103 Sisak, Croatia. Tel.: +385 44 533 380; fax: +385 44 533 379.
E-mail address: brnardic@simet.hr (I. Brnardić).

0272-8842/$ - see front matter © 2013 Elsevier Ltd and Techna Group S.r.l. All rights reserved.
http://dx.doi.org/10.1016/j.ceramint.2013.05.063

[1,4]. To date, research on detailed surface functionalization of NaTiNTs and NaTiNRs with APTES has not been reported.

In this paper, NaTiNTs and NaTiNRs were functionalized by APTES molecules. Modifications were performed during different time intervals and with the use of various amounts of APTES. In addition, two different ways of functionalization were performed: conducting the prehydrolization of APTES molecules before the functionalization of nanoparticles and using APTES as received. The main objective for conducting this investigation was to examine possibilities of functionalization and to determine how different reaction conditions influence the functionalization of NaTiNTs and NaTiNRs. To our knowledge, until now this type of detailed research on the functionalization of NaTiNTs and NaTiNRs has not been carried out. Functionalized nanoparticles will be further used to prepare polymer/functionalized TiO_2 nanocomposites. Similarly, functionalized nanoparticles could enhance polymer/functionalized TiO_2 interactions and improve mechanical properties as shown by Byrne et al. [1].

2. Experimental

2.1. Synthesis of starting materials

Sodium TiO_2 nanotubes (NaTiNTs) and TiO_2 nanoribbons (NaTiNRs) were synthesized at 115 and 175 °C respectively under hydrothermal conditions from anatase TiO_2 and 10 M NaOH(*aq*). Isolated NaTiNTs and NaTiNRs were dried at 300 °C to remove interlayer and surface water [17].

2.2. Functionalization of synthesized sodium TiO_2 nanostructures

For functionalization a commercially available 3-(aminopropyl) triethoxysilane (APTES) was supplied by Sigma-Aldrich. Materials were used as received.

The functionalization of nanoparticles was performed in two different ways: (i) first, 1 g of NaTiNTs or NaTiNRS was dispersed in a mixture of 300 cm^3 absolute ethanol and APTES (30 wt% per NaTiNTs/NaTiNRs). Prepared mixture was stirred on a magnetic stirrer and at the same time it was sonicated with an ultrasonic probe for different periods of time (2, 4 and 24 h) at room temperature. NaTiNTs/NaTiNRs were also functionalized with different amounts of APTES (60 and 100 wt% per NaTiNTs/NaTiNRs). In this case, the prepared mixtures were stirred and sonicated for 24 h. The solid phases of the functionalized NaTiNTs/NaTiNRs were separated by centrifugation and then washed four times with absolute ethanol and dried under a vacuum at 40 °C for 24 h. (ii) Following the second functionalization strategy, APTES was first prehydrolized in 300 cm^3 of water–ethanol solution (vol. ratio 50:50) and hydrochloric acid as a catalyst. This solution was mixed on a magnetic stirrer for 2 h at 60 °C when 1 g of NaTiNTs/NaTiNRs was added in a ratio according to APTES content (30 wt% per NaTiNTs/NaTiNRs). The resulting mixture was stirred and sonicated for an additional period of time (2, 4 and 24 h). In addition, NaTiNTs/NaTiNRs were functionalized using different contents of prehydrolized APTES (60 and 100 wt% per nanoparticles). These prepared mixtures were stirred and sonicated for 24 h. Once the reactions had finished, solid phases were isolated by centrifugation. The isolated centrifuged and solid phases were washed four times with ethanol. Finally, the separated phases were dried under a vacuum at 40 °C for 24 h.

2.3. Characterization of functionalized nanoparticles

A simultaneous differential scanning calorimetry-thermogravimetric analysis (DSC-TGA) was carried out on a Metller Toledo TGA/DSC1 StarSystem operating in an oxygen atmosphere, at a heating rate of 10 K min^{-1}, with a sample size ~10 mg. To determine the degradation properties and weight loss of nanoparticles after the functionalization, each sample was scanned from 40 to 1000 °C.

Infrared spectra were recorded using a Fourier transform infrared (FTIR) spectrometer on a Perkin-Elmer spectrum one, equipped with an attenuated total reflection (ATR) accessory with a diamond crystal in the range from 4000 to 400 cm^{-1}. Each spectrum was averaged over 16 scans at a resolution of 4 cm^{-1}.

The functionalized NaTiNTs and NaTiNRs were checked with a Supra 35LV scanning electron microscope (SEM) operating at 1 kV. The presence of APTES grafting on the nanoparticles was determined by using an energy dispersion spectroscopy (EDS) mapping analysis. Samples for SEM characterization were prepared by placing the functionalized NaTiNTs and NaTiNRs on a sample holder covered with a piece of double-sided carbon conductive tape. The sample particles were then carbon-coated.

3. Results and discussion

3.1. Thermal properties

The decomposition behavior of all samples was examined by simultaneous DSC-TGA analysis as shown in Figs. 1 and 2. To allow a better comparison of the results, NaTiNTs and NaTiNRs were identically treated as functionalized NaTiNTs and NaTiNRs, only without APTES.

Fig. 1 compares as-synthesized NaTiNRs and NaTiNRs functionalized with 100 wt% of prehydrolized APTES. Although the weight loss in the temperature range of 40–300 °C is almost the same for both samples, it is the DSC signal which shows a significant difference and confirms the modification. The mass loss below 220 °C and two endothermic peaks at 120 and 180 °C can be attributed to the loss of water and further condensation of APTES. Further loss at a temperature range of 250–500 °C with an exothermic peak at 285 °C can be assigned to the decomposition of aminopropyl groups from the nanoparticles. Since the degradation temperature of APTES grafted on nanoparticles is higher than the boiling temperature of APTES, 217 °C, we can assume that there was chemical bonding between the functionalized nanoparticles, NaTiNTs and NaTiNRs, and APTES [18–22]. The presence of an exothermic peak at

800 °C can be attributed to the recrystallization of titanates which is a consequence of functionalization.

The weight loss of residue at 1000 °C increases with the loading of APTES (Fig. 2 and Table 1). As can be seen, the time for functionalization with 30 wt% of APTES does not significantly influence the amount of grafted APTES on the NaTiNTs. It is thus evident that a period of 2–4 hours is enough time for functionalization of NaTiNTs and NaTiNRs with prehydrolized APTES.

Further, functionalized NaTiNTs show a bigger weight loss which implies a higher content of the grafted APTES molecules on the nanotubes. It can be argued that NaTiNRs are dimensionally bigger than NaTiNTs which reduces the surface and number of active sites for grafting of the APTES molecules.

It is notable that, where the NaTiNRs were functionalized for a longer time with 30 wt% of non-prehydrolized APTES, the weight loss at 1000 °C decreases from 12.6% for 2 h to 10.5% for 24 h (Table 1). This can also be explained by the APTES molecules firstly bonding through the hydrolization of one ethoxy group on the NaTiNRs and then the other two ethoxy groups with the NaTiNRs or another silane molecule bound in the vicinity. The result is a smaller weight loss at 1000 °C for the sample functionalized for 24 hours due to the smaller content of ethoxy groups that could thermally degrade. That result is in accordance with the FTIR measurements explained later in the text.

In addition, the NaTiNTs and NaTiNRs functionalized with prehydrolized APTES show a greater weight loss in comparison with the NaTiNTs and NaTiNRs functionalized with non-prehydrolized APTES (Table 1). It is well known that APTES reacts through sol–gel polymerization that depends on the catalysis, temperature, amount of water and solvent. The sol–gel process consists of two reactions, namely hydrolysis and condensation [23]. During this experiment, prehydrolization under acid condition at pH 1 and 60 °C was performed. The reaction of the acid catalyzed hydrolysis is faster than polycondenzation and not strongly influenced by the degree of silica condensation [23,24]. In the first stage of the hydrolysis all monomers react and form cyclic structures which gradually condensate to an open, weakly branched structure. Such prehydrolized APTES molecules can bond more easily with nanoparticles, NaTiNTs and NaTiNRs compared to non-prehydrolized APTES.

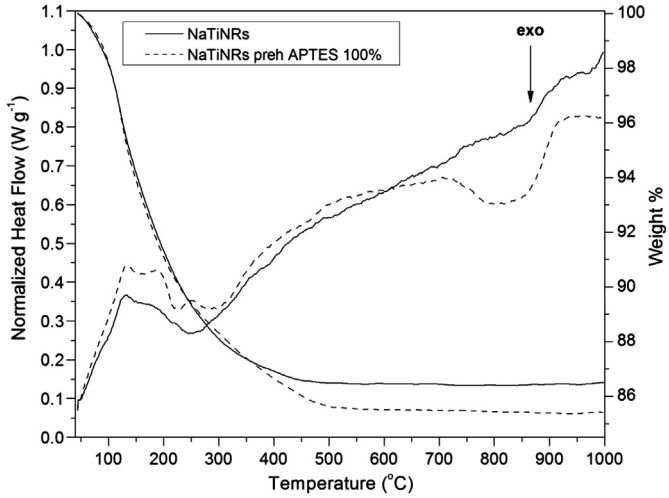

Fig. 1. Dynamic DSC thermograms and TGA curves of the NaTiNRs and NaTiNRs functionalized with prehydrolized APTES for 24 h with 100 wt%

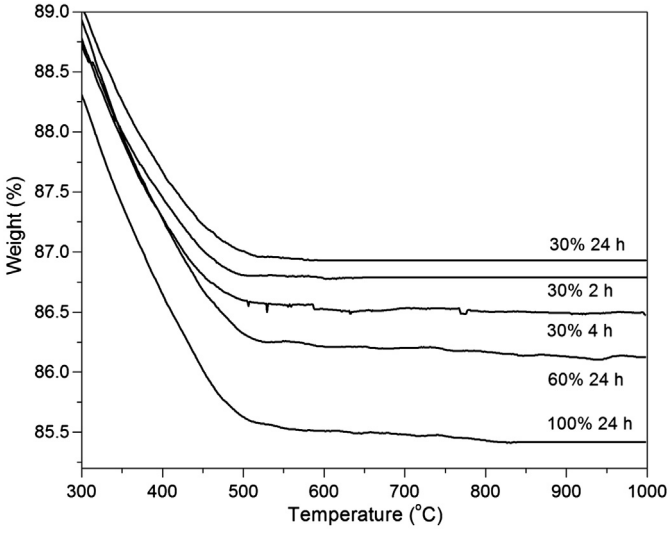

Fig. 2. TGA curves for the NaTiNRs functionalized at different times (2, 4 and 24 h) with 30 wt% and with 60 and 100 wt% of prehydrolized APTES for 24 h.

3.2. FTIR analysis

Figs. 3 and 4 show the FTIR results of systems obtained at different conditions. In the FTIR spectrum of APTES, the band at 1470 and 1450 cm^{-1} can be assigned to the bending vibrations of C–H band in the propyl group [18], while the band at 1440 cm^{-1} can be ascribed to the asymmetric and

Table 1
Weight loss (%) at 1000 °C for investigated systems.

Systems				
Content of APTES and functionalization time	NaTiNTs+non-preh. APTES	NaTiNTs+preh. APTES	NaTiNRs+non-preh. APTES	NaTiNRs+preh. APTES
30 wt%—2 h	14.6	15.6	12.6	13.2
30 wt%—4 h	14.4	15.3	12.0	13.5
30 wt%—24 h	14.9	15.4	10.5	13.1
60 wt%—24 h	15.7	17.7	11.0	13.9
100 wt%—24 h	16.0	17.5	10.9	14.6

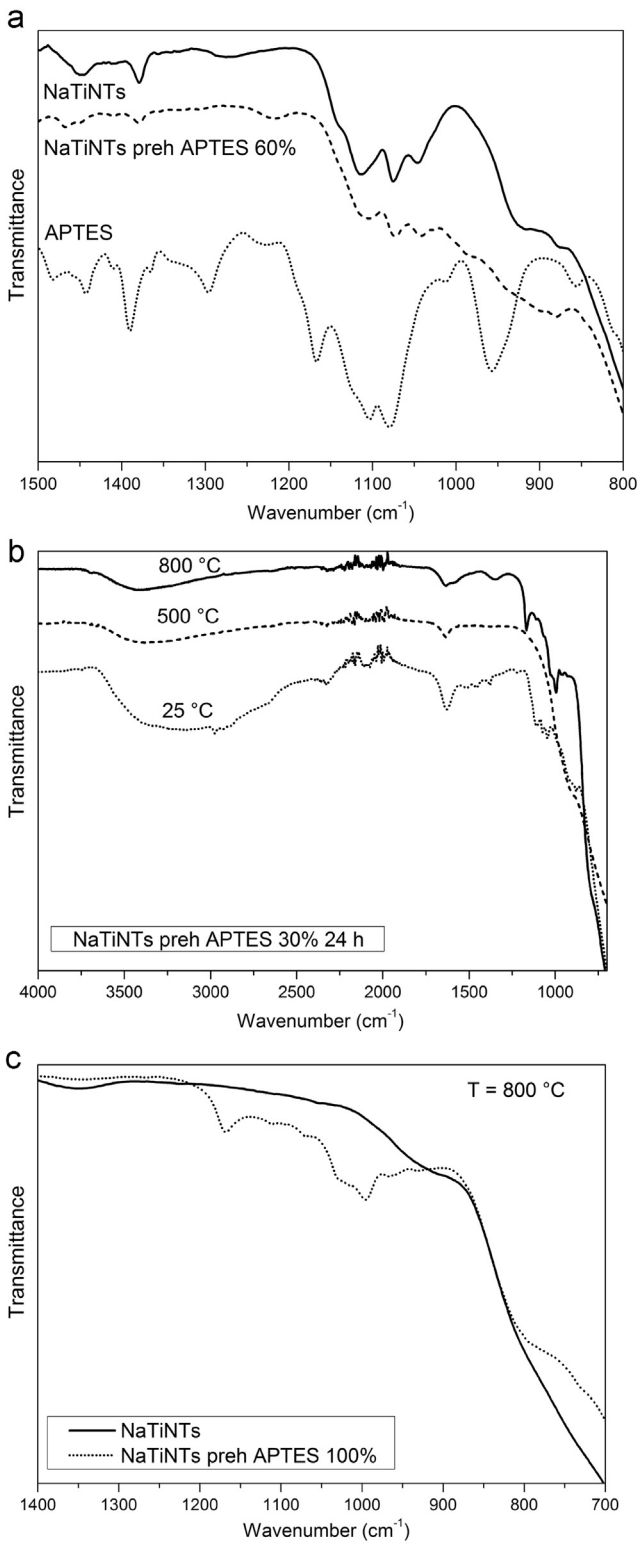

Fig. 3. FTIR spectra of: a) as-synthesized NaTiNTs, NaTiNTs functionalized with 60 wt% of prehydrolized APTES and APTES; b) the NaTiNTs functionalized with 30 wt% of prehydrolized APTES for 24 h *vs.* temperature; and c) as-synthesized NaTiNTs and NaTiNTs functionalized with 100 wt% of prehydrolized APTES annealed at 800 °C.

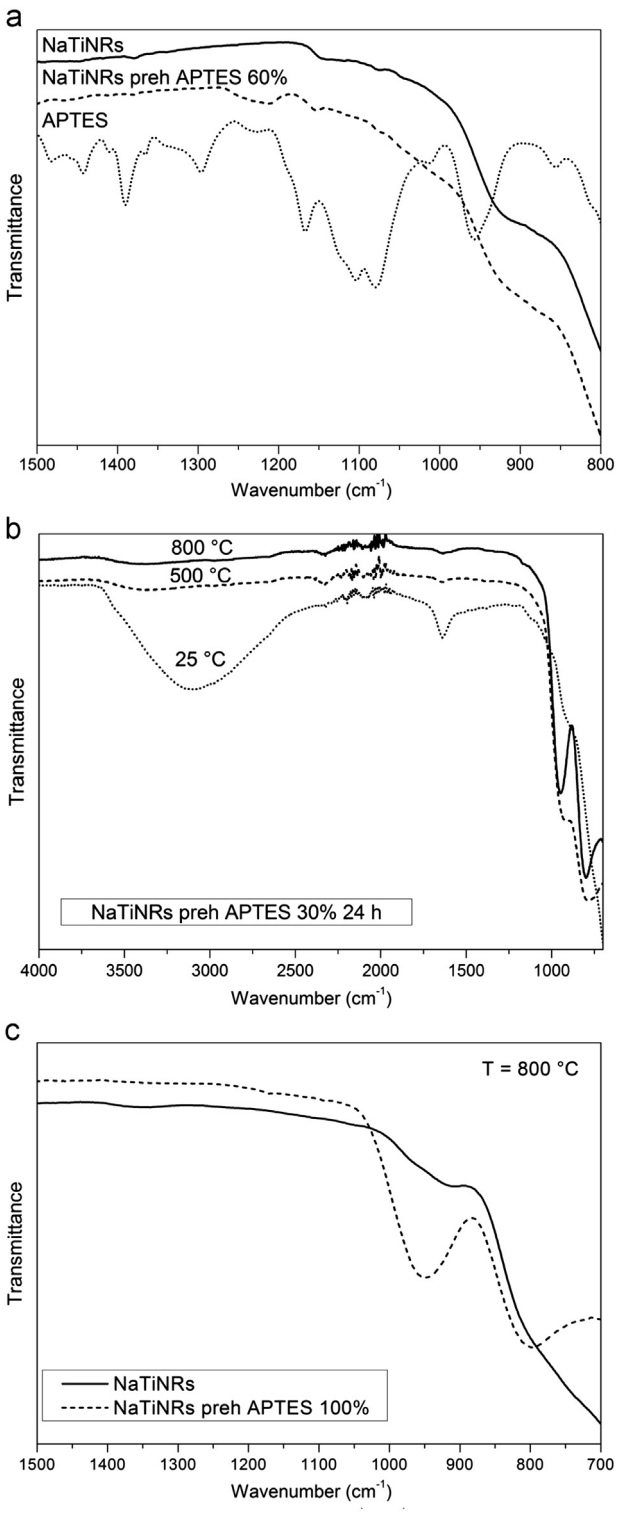

Fig. 4. FTIR spectra of: a) as-synthesized NaTiNRs, NaTiNRs functionalized with 60 wt% of prehydrolized APTES and APTES; b) the NaTiNRs functionalized with 30 wt% of prehydrolized APTES for 24 h *vs.* temperature; and c) as-synthesized NaTiNRs and NaTiNRs functionalized with 100 wt% of prehydrolized APTES at 800 °C.

symmetric deformation of the CH_3 group from the ethoxy group [25] (Fig. 3a). Similar bands at 1480 and 1450 cm^{-1} appear in the NaTiNTs functionalized with 60 wt% of prehydrolized APTES, confirming the presence of prehydrolized APTES on the NaTiNTs. The band at 1215 cm^{-1} is attributed to the vibration bands of Si–O–Si groups [19,22,26].

The appearance of overlapped bands in the region 900–1000 cm^{-1} for the functionalized NaTiNTs samples indicates the development of an inorganic–organic connection during functionalization of the NaTiNTs with prehydrolized APTES. Those bands can be assigned to the Ti–O—Si bonds vibration superimposed to stretching vibrations of Si–O^- or Si–OH groups [7,27]. Similar FTIR results for NaTiNRs systems are shown in Fig. 4a.

Fig. 3b shows the spectra of functionalized NaTiNTs with 30 wt% prehydrolized APTES for 24 h after functionalization (25 °C) compared to the same sample with different heat treatment, at 500 and 800 °C. The wide band at ~3400 cm^{-1} attributed to OH stretching reduces when the sample is heated. At a temperature of 500 °C overlapping bands in the region of 900–1240 cm^{-1} appear. They can be assigned to Si–O–Si asymmetric stretching, the vibration of Ti–O–Si bonds and to stretching vibrations of the Si–O^- or Si–OH groups as mentioned previously. After treatment at 800 °C, bands at 1165 and 1000 cm^{-1} due to Si–O–Si are observed. The band at 950 cm^{-1} is attributed only to the stretching vibration of the Ti–O–Si group [7,28,29]. Further, when comparing the FTIR spectra of the as-synthesized NaTiNTs with the functionalized NaTiNTs with 100 wt% of prehydrolized APTES annealed at 800 °C, the same results appear (Fig. 3c). The shoulder at 800 cm^{-1} can be assigned to the symmetric stretching of the Si–O–Si [7]. The FTIR results in Fig. 4b and c are similar to those in Fig. 3b and c. A small difference can be found in the almost complete disappearance of the band at 1640 cm^{-1} with heat treatment attributed to the NH_2 asymmetric bending. It is interesting to note that the bands at 950 and 800 cm^{-1}, assigned to the Ti–O–Si and Si–O–Si groups after heat treatment at 800 °C, are more pronounced in Fig. 4b and c than in Fig. 3b and c.

The same conclusion may be drawn from the FTIR results of the NaTiNTs and NaTiNRs functionalized with non-prehydrolized APTES (not shown).

The FTIR spectra of the NaTiNRs functionalized with 30 wt % of non-prehydrolized APTES for 2, 4 and 24 h are shown in Fig. 5. The bands around 1440 and 1380 cm^{-1} can be assigned to the asymmetric and symmetric deformation of the CH_3 groups from the ethoxy moieties of APTES. With a longer functionalization time, the band at 1380 cm^{-1} is reduced and the broad peak around 1450 cm^{-1} becomes more pronounced. The absorption band at 1460 cm^{-1} corresponds to the NH_2 groups of the APTES molecules. Hydrolization of the ethoxy occurs and NH_2 groups of the APTES molecules become more pronounced with a time of 24 h for functionalization [25]. The results correspond to the TGA results, as mentioned previously.

3.3. SEM–EDS mapping

After the functionalization, the grafting of the APTES molecules on the NaTiNTs and NaTiNRs was investigated by an SEM–EDS mapping analysis of Ti, O, Si and N across a selected surface area in all functionalized NaTiNRs and NaTiNTs. Fig. 6 shows a SEM image of the NaTiNRs functionalized with 100 wt% of non-prehydrolized APTES

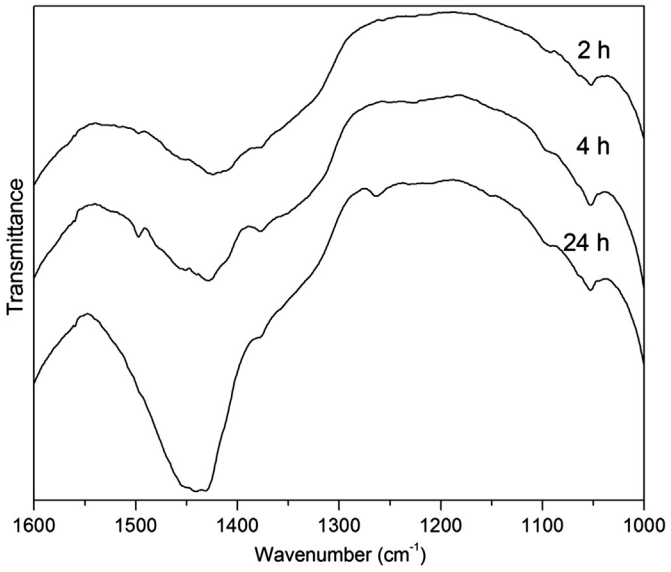

Fig. 5. FTIR spectra of the NaTiNRs functionalized with 30 wt% of non-prehydrolized APTES for 2, 4 and 24 h.

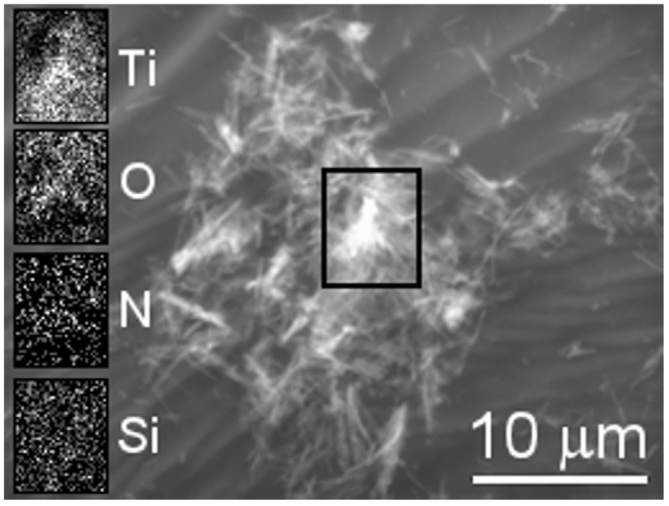

Fig. 6. SEM–EDS image of the NaTiNRs functionalized with 100 wt% of non-prehydrolized APTES with the corresponding mapping analysis of the Ti, O, Si and N mapping. The frame in the SEM image shows the analyzed area.

with corresponding element maps. Mapping analysis of Si and N revealed the existence of APTES molecules on the NaTiNRs which is in line with the results obtained from the DSC-TGA and FTIR measurements. Similar results were found for all the functionalized NaTiNRs/NaTiNTs samples (not shown).

4. Conclusions

Both pristine as well as prehydrolized APTES molecules were successfully used for the surface functionalization of the NaTiNTs and NaTiNRs, which was confirmed by using various characterization techniques.

The DSC-TGA results show the degradation of the APTES molecules on the functionalized NaTiNTs/NaTiNRs samples and that the weight loss at 1000 °C increases with the loading of APTES. It was found that a period of up to 4 h is long enough for the successful functionalization of the NaTiNRs with prehydrolized APTES and as well for the functionalization of the NaTiNTs with and without prehydrolization of APTES. It is noted that with longer functionalization times of the NaTiNRs with 30 wt% of non-prehydrolized APTES the weight loss at 1000 °C decreases. It is thus concluded that the functionalization time should exceed 4 h. This result is in accordance with the FTIR measurements. In addition, the FTIR measurements confirm the Ti–O–Si bonding in all samples. The existence of APTES molecules on the nanoparticles was confirmed by the SEM–EDS analysis.

Acknowledgments

The authors acknowledge the financial support of the Ministry of Education, Science, Culture and Sport of the Republic of Slovenia under contract No. 3211-10-000057 (Center of Excellence Polymer Materials and Technologies) and project J2-4034, the Ministry of Science, Education and Sports of the Republic of Croatia through the research project "Bioceramic, Polymer and Composite Nanostructured Materials" (125-1252970-3005) and the European Commission through COST project action no. MP0902 "Composites of Inorganic Nanotubes and Polymers (COINAPO)".

References

[1] M.T. Byrne, J.E. McCarthy, M. Ben, R. Blake, Y.K. Gun'ko, E. Horvath, Z. Konya, A. Kukovecz, I. Kiricsi, J.N. Coleman, Chemical functionalisation of titania nanotubes and their utilisation for the fabrication of reinforced polystyrene composites, Journal of Materials Chemistry 17 (2007) 2351–2358.

[2] Z. Shi, G. Xueping, S. Deying, Y. Zhou, D. Yan, Preparation of poly (3-caprolactone) grafted titanate nanotubes, Polymer 48 (2007) 7516–7522.

[3] H.-J. Song, Z.-Z. Zhang, X.-H. Men, Tribological behavior of polyurethane-based composite coating reinforced with TiO_2 nanotubes, European Polymer Journal 44 (2008) 1012–1022.

[4] P. Umek, M. Huskić, A. Sever Škapin, U. Florjančič, B. Zupančič, I. Emri, D. Arčon, Structural and mechanical properties of polystyrene nanocomposites with 1D titanate nanostructures prepared by an extrusion process, Polymer Composites 30 (2009) 1318–1325.

[5] H. Shi, F. Liu, L. Yang, E. Han, Characterization of protective performance of epoxy reinforced with nanometer-sized TiO_2 and SiO_2, Progress in Organic Coatings 62 (2008) 359–368.

[6] Y. Lai, Y. Chen, Y. Tang, D. Gong, Z. Chen, C. Lin, Electrophoretic deposition of titanate nanotube films with extremely large wetting contrast, Electrochemistry Communications 11 (2009) 5268–2271.

[7] G. Brusatin, M. Guglielmi, P. Innocenzi, A. Martucci, G. Battaglin, S. Pelli, G. Righini, Microstructural and optical properties of sol–gel silica–titania waveguides, Journal of Non-Crystalline Solids 220 (1997) 202–209.

[8] L. Valentini, J. Macan, I. Armentano, F. Mengoni, J.M. Kenny, Modification of fluorinated single-walled carbon nanotubes with aminosilane molecules, Carbon 44 (2006) 2196–2201.

[9] J. Zhu, M. Yudasaka, M. Zhang, D. Kasuya, S. Iijima, A surface modification approach to the patterned assembly of single-walled carbon nanomaterials, Nano Letters 3 (2003) 1239–1243.

[10] Q. Fu, C. Lu, J. Liu, Selective coating of single wall carbon nanotubes with thin SiO_2 layer, Nano Letters 2 (2002) 329–332.

[11] M. Alexandre, P. Dubois, Polymer-layered silicate nanocomposites: preparation, properties and uses of a new class of materials, Materials Science Engineering: R: Reports 28 (2000) 1–63.

[12] S.T. Hussain, A. Siddiqa, M. Siddiq, S. Ali, Iron-doped titanium dioxide nanotubes: a study of electrical, optical, and magnetic properties, Journal of Nanoparticle Research 13 (2011) 6517–6525.

[13] K. Hashimoto, H. Irie, A. Fujishima, TiO_2 photocatalysis: a historical overview and future prospects, Japanese Journal of Applied Physics 44 (2005) 8269–8285.

[14] U. Diebold, The surface science of titanium dioxide, Surface Science Reports 48 (2003) 53–229.

[15] T. Kasuga, M. Hiramatsu, A. Hoson, T. Sekino, Titania nanotubes prepared by chemical processing, Advanced Materials 11 (1999) 1307–1311.

[16] M. Humar, D. Arčon, P. Umek, M. Škarabot, I. Muševič, G. Bregar, Mechanical properties of titania-derived nanoribbons, Nanotechnology 17 (2006) 3869–3872.

[17] P. Umek, R. Cerc Korošec, B. Jancar, R. Dominko, D. Arcon, The influence of the reaction temperature on the morphology of sodium titanate 1D nanostructures and their thermal stability, Journal of Nanoscience and Nanotechnology 7 (2007) 3502–3508.

[18] S.-C. Shen, W.K. Ng, L. Chia, Y.-C. Dong, R.B.H. Tan, Sonochemical synthesis of (3-aminopropyl)triethoxysilane-modified monodispersed silica nanoparticles for protein immobilization, Materials Research Bulletin 46 (2011) 1665–1669.

[19] H. Kim, J.C. Jung, S.H. Yeom, K.-Y. Lee, J. Yi, I.K. Song, Immobilization of a heteropolyacid catalyst on the aminopropyl-functionalized mesostructured cellular foam (MCF) silica, Materials Research Bulletin 42 (2007) 2132–2142.

[20] X. Liu, Y. Hua, G. Villemure, Preparation and characterization of thin films of amine functionalised mesoporous silica having cubic pore structures and their use for electrode surface modifications, Microporous and Mesoporous Materials 117 (2009) 317–325.

[21] X. Wang, Y.-H. Tseng, J.C.C. Chan, S. Cheng, Direct synthesis of highly ordered large-pore functionalized mesoporous SBA-15 silica with methylaminopropyl groups and its catalytic reactivity in flavanone synthesis, Microporous and Mesoporous Materials 85 (2005) 241–251.

[22] X. Zhang, W. Wu, J. Wang, X. Tian, Direct synthesis and characterization of highly ordered functional mesoporous silica thin films with high amino-groups content, Applied Surface Science 254 (2008) 2893–2899.

[23] J. Macan, Synthesis and Characterization of Organic–Inorganic Interpenetrating Polymer Networks (Ph.D. thesis), Faculty of Chemical Engineering and Technology, University of Zagreb, Zagreb, 2006 (in Croatian).

[24] L.V. Ng, P. Thompson, J. Sanchez, C.W. Macosko, A.V. McCormick, Formation of cagelike intermediates from nonrandom cyclization during acid-catalyzed sol–gel polymerization of tetraethyl orthosilicate, Macromolecules 28 (1995) 6471–6476.

[25] J. Kim, P. Seidler, L.S. Wan, C. Fill, Formation, structure, and reactivity of amino-terminated organic films on silicon substrates, Journal of Colloid and Interface Science 329 (2009) 114–119.

[26] I.A. Rahman, M. Jafarzadeh, C.S. Sipaut, Silylation of multi-walled carbon nanotubes, Ceramics International 368 (2003) 121–124.

[27] R. Mendoza-Serna, P. Bosch, J. Padilla, V.H. Lara, J. Méndez-Vivar, Homogeneous Si–Ti and Si–Ti–Zr polymeric systems obtained from monomeric precursors, Journal of Non-Crystalline Solids 217 (1997) 30–40.

[28] S. Portal, R.M. Almeida, Variable incidence infrared absorption spectroscopy of gel-derived silica and titania films, Physica Status Solidi A 201 (2004) 2941–2947.

[29] Z. Jiwei, Z. Liangying, Y. Xi, S.N.B. Hodgson, Characteristics of laser-densified and conventionally heat treated sol–gel derived silica-titania films, Surface and Coatings Technology 138 (2001) 135–140.